Proceedings of the ASME 2017 International Design Engineering Technical Conferences & Computers and Information in Engineering Conference
IDETC2017
August 6-9, 2017, Cleveland, Ohio, USA

IDETC2017-68105

POINT-BASED SHAPE MONITORING OF PLATE BENDING FOR LARGE-SCALE STORAGE TANKS

Kenta Fukano
IHI Corpolation
Isogo-ku, Yokohama, Japan

Hiroshi Masuda
The University of Elector-Communications
Chofu, Tokyo, Japan

Ataru Kobayashi
The University of Elector-Communications
Chofu, Tokyo, Japan

Kazuki Ikeda
IHI Corpolation
Isogo-ku, Yokohama, Japan

ABSTRACT

Storage tanks are constructed using thousands of large curved steel plates, which are manufactured from flat plates. In conventional manufacturing of curved plates, operators fit wooden templates to specific positions on steel plates and measure differences between the current shape and the template. However, it is costly to create many wooden templates for a variety of plates. In addition, it is time-consuming and requires skills to precisely place wooden templates on specific positions to measure differences. In this paper, we discuss methods to automatically calculate differences of shapes during bending processes without wooden templates. We capture dense points on steel plates using a terrestrial laser scanner, and analyze shapes of curved plates using point-clouds. In our method, the system extracts only the points on curved plates, and tracks the amount of deformation on reference lines defined on the plates. Corresponding positions between intermediate curved plates and the original flat shape are calculated using mesh flattening techniques. In our experiments, our method could calculate the amount of differences of steel plates in reasonable performance and precision.

1. INTRODUCTION

Large storage tanks, which are used for storing gas or liquid, have diameters of more than fifty meters. They are constructed by welding thousands of curved steel plates. It takes a very long time to manufacture many curved steel plates. The shapes of storage tanks are typically bodies of revolution, and curved plates are cylinders, spheres, cones or tori. Each plate has thickness of more than three centimeters.

In constructing a large storage tank, plates are usually bended using a large press machine. Since the number of plates is very large, time-consuming line heating is rarely used. Each plate varies from 2 to 5m in length. To manufacture a flat rectangle plate to the desired curved shape, operators have to gradually bend the plate in trial-and-error by using a press machine many times. It is strongly required to efficiently manufacture curved plates to reduce construction period of storage tanks.

The storage tanks are built to order, and the specifications are different each time. So, it is not reasonable to product molds for specific plates. Instead, a movable die is used for bending the plates, as shown in Figure1. To manufacture curved plates, operators select types of dies and decide their positions on the table of a press machine. Then operators bend the plate with a very heavy weight. Since operators can bend only a small amount at a time, they have to do the operations a large number of times while changing types and positions of dies.

Operators estimate adequate types and positions of dies by fitting wooden templates to specific positions on a curved plate. However, it is costly to generate many wooden templates, and it is also time-consuming to confirm the amount of deformation using wooden templates at each operation. In addition, the quality and efficiency of plate-bending heavily depend on skills of operators. For skill transfer from experts, it is important to analyze bending process and convert tacit knowledge into formal one.

In order solve these problems, we will develop a computerized system, which automatically measures the amount of deformation of curved plates without wooden templates, and enables operators to make decisions on bending processes based on the calculated results.

To measure 3D shapes of large plates, a terrestrial laser scanner is useful. So far, many researchers have studied methods for reconstructing 3D models of large-scale facilities from point-clouds captured using terrestrial laser scanners [1-4]. Sun, et al. calculated shapes of steel plates for shipbuilding based on point-clouds[5]. Joo, et al. also calculated plate shapes based on differential geometry [6]. However, their methods are time-consuming for processing in real time on site. We require more efficient processing methods for large-scale point-clouds.

Typical terrestrial laser scanners emit laser beams to objects, and measure the round-trip travel time. Since the direction of a laser beam is known and the round-trip distance can be calculated from the speed of light, 3D coordinates on objects can be obtained using the distance and the direction. In this paper, we used FARO Focus 3D S120, which is a phase-based terrestrial laser scanner. This laser scanner can capture one million points per second within 100m.

Figure 2 shows the arrangement of a laser scanner, a steel plate, and a press machine. When each bending operation is finished, the laser scanner captures a dense point-cloud in a region containing the steel plate. Then the point-cloud is transferred to the computer, and the shape of the curved plate is analyzed. The result is displayed on the screen of the computer.

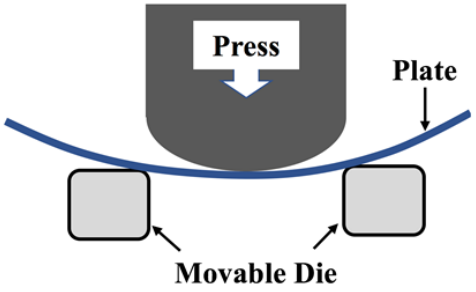

Figure 1. Press machine

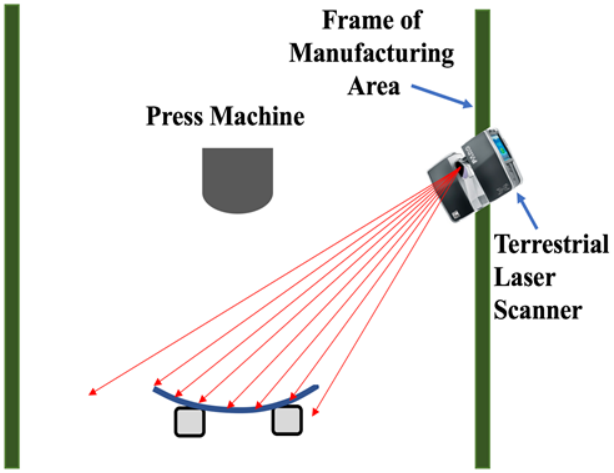

Figure 2. Configuration for measurement

2. OVERVIEW

Figure 3 illustrates a process of plate-bending operations based on our system. After operators deform a steel plate using a press machine, the point-cloud of the plate is captured using a terrestrial laser scanner. Since a raw point-cloud includes unnecessary points on floors, walls and the machine tool, the system extracts only the points on the curved plate. Then we detect a boundary loop and corner points of the rectangle plate. Then the system generates a rough mesh model of the plate. Since the number of points is too large to process in a short time, the number of vertices on the mesh model is reduced to an appropriate number.

Then the mesh model is mapped on the original flat shape of the plate using mesh flattening techniques. Parameter (u, v) is defined on the horizontal plane, and the parameter is attached to each point on the mesh model.

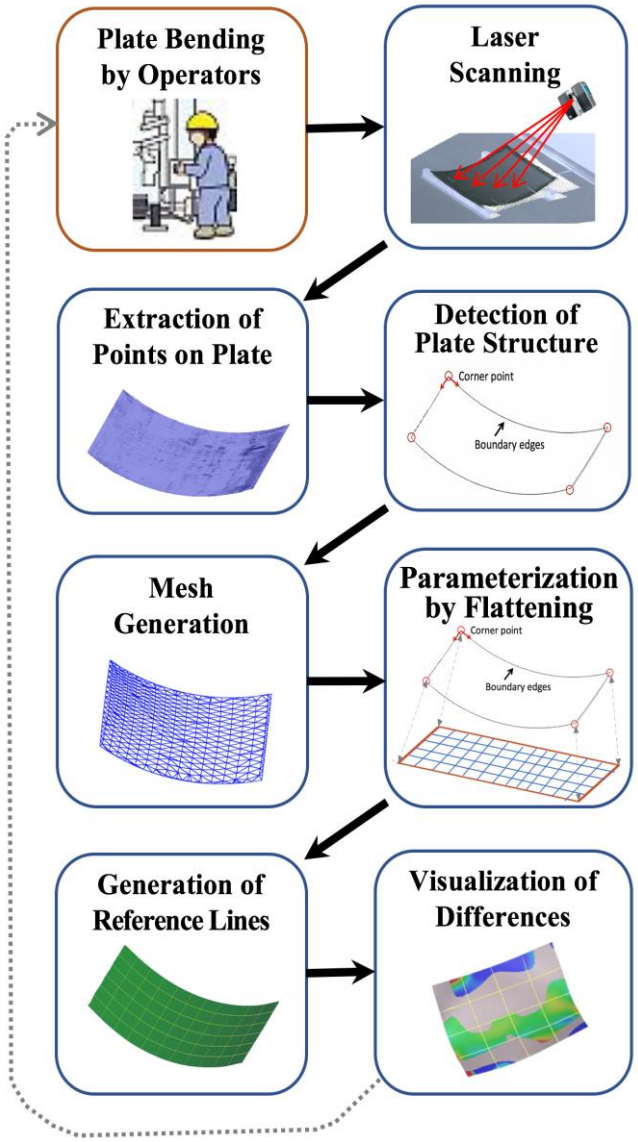

Figure 3. Process for measuring steel plates

The parameters are used for identifying correspondent positions on different shapes in bending process. The system calculates differences between plate shapes before and after bending, using parameters (u, v). The differences are shown to operators for supporting decision making on plate-bending process. Since parameters (u, v) are obtained, geometric properties, such as curvature, can be easily calculated by fitting a B-spline surface to points on the plate.

3. EXTRACTION OF PLATES FROM POINT-CLOUD

3.1. Extraction of a plate on the stage

The terrestrial laser scanner captures a broad range of points in a factory. Figure 4 shows an example of a point-cloud, which contains various objects, such as walls, floors, a press machine, control units, and operators. It is necessary to extract only the points on the steel plate.

The laser scanner emits laser beams by rotating the mirror in the attitude and azimuth angles, as shown in Figure 5. 3D coordinates are expressed in the scanner-centered coordinate system. Since points are measured at the equal angle intervals, the spherical coordinates (θ, ϕ, r) are ordered on the θ-ϕ plane in a lattice manner [3,4], as shown in Figure 6(a).

We detect points on the plate on this 2D lattice. First, we divide points into continuous regions, as shown in Figure 6(b). Suppose that the constant angle interval is δ [radian], and the angle between the surface normal and the laser beam is α_i at point $\mathbf{p}_i$. Because points are densely measured, δ is very small. Then we can approximate the distance between adjacent points $\mathbf{p}_1$ and $\mathbf{p}_2$ on the plate as:

$$\frac{(|\mathbf{p}_1| + |\mathbf{p}_2|)\delta}{2\cos\{(\alpha_1 + \alpha_2)/2\}} \quad (1)$$

Figure 4. Point-cloud containing a steel plate

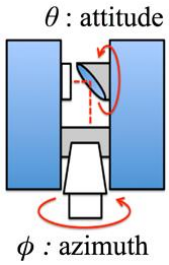

Figure 5. Angles of laser beams

Since α cannot be a right angle on the steel plate, we suppose $\alpha < 0.4\pi$. Then adjacent points $\mathbf{p}_1$ and $\mathbf{p}_2$ are on the same surface if they satisfy:

$$\left|\mathbf{p}_1\right| + \left|\mathbf{p}_2\right| < 1.62(|\mathbf{p}_1| + |\mathbf{p}_2|)\delta \quad (2)$$

In Figure 6(b), the steel plate is extracted as a continuous region. Since the plate is placed on movable dies, it can be separated from the table of the press machine using the continuity criteria of Equation 2.

Since storage tanks are made of thick steel plates, the continuous region of a steel plate often includes side surfaces of the plate, as shown in Figure 7(a). To eliminate side surfaces, we calculate the normal vector at each point, and extract a smooth surface using the region growing method. Since points are noisy, they are smoothed using the low-pass filter [7] before normal vectors are calculated. Figure 7(b) shows an extracted smooth surface.

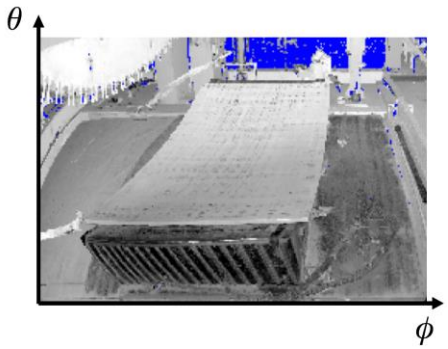

(a) Points are ordered on θ-ϕ.

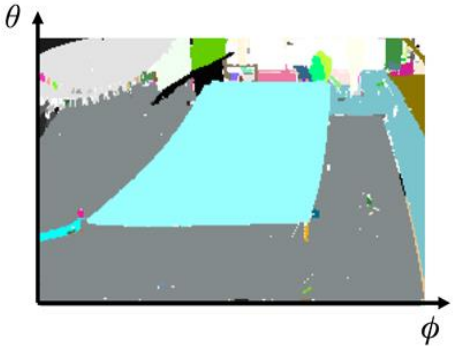

(b) Continuous regions

Figure 6. Segmentation of point-cloud

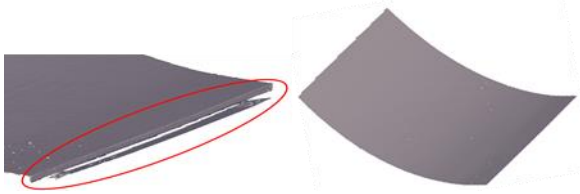

(a) Side surface (b) Extracted plate surface

Figure 7. Extraction of a smooth surface

3.2. Extraction of boundary of plate

When points on a plate are successfully extracted, they are converted into a mesh model. Since points are ordered in a lattice manner, a mesh model can be easily generated by connecting adjacent points on the θ-ϕ plane.

We detect a boundary loop of the steel plate. Figure 8(a) shows boundary edges of a mesh model. Generally multiple loops exist on the boundary because of noises and missing points. So, we detect the longest loop on the boundary edges. In our method, we select an edge and traverse the shortest path from the both ends of the edge, as shown in Figure 8(b). The shortest path is searched using the Dijkstra algorithm. This process is repeated until a sufficiently long loop is obtained.

Then, the four corner points of the rectangle plate are calculated using a boundary loop. To stably calculate corner points, we select the k-th neighbor points in both directions of each edge, and calculate their angle, as shown in Figure 9(a). We regard an edge is the candidate of corner points when the angle θ are less than a threshold. In our research, we specified $\theta < 150°$ and $k = 128$. Figure 9(b) shows candidate points.

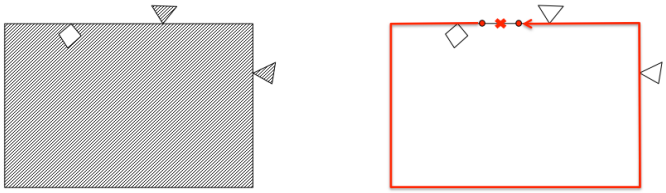

(a) Boundary edges of a plate (b) The shortest path

(c) A closed loop of the plate

Figure 8. Detection of a closed loop

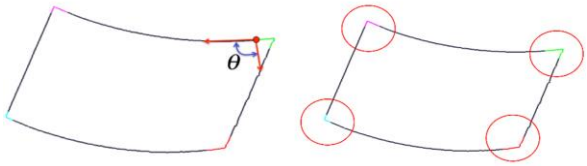

(a) Angle of neighbor points (b) Candidates of corners

(c) Intersection point (d) Corner points

Figure 9. Detection of corner points

Then we detect straight lines using the RANSAC method, and calculate the intersection points, as shown in Figure 9(c). Finally, four corner points can be calculated, as shown in Figure 9(d).

When four corner points are detected, the boundary loop is divided into four lines, which represent edges of the rectangle steel plate. Since each boundary edge is noisy, we smooth edges by fitting a B-spline curve. In Figure 8, four edges of the steel plate are represented as smooth B-spline curves.

4. COMPARISON OF PLATE SHAPES ON REFERENCE LINES

4.1 Approach for tracking reference lines on the plate

The shape of a steel plate is gradually deformed according to iterative press operations. In actual operations, reference points or lines are defined on the plate before bending operations begin, as shown in Figure 10(a). When the plate is bended, a wooden pattern is placed on the reference position and the amount of deformation is investigated. However, it is time-consuming and tedious work to precisely draw lines on plates, and carefully place wooden templates on the lines.

In our research, we track positions of virtual reference lines on curved steel plates. Virtual reference lines are initially defined on a flat steel plate. When the steel plate is bended, the shape of the curved plate is reconstructed from points, and it is mapped onto the original rectangle shape, as shown in Figure 10(b). Then reference lines on the original shape are copied to the curved plate.

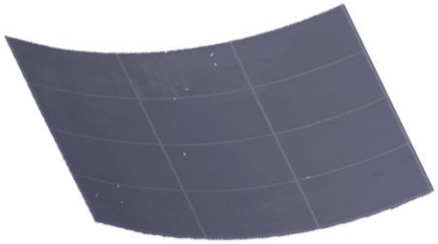

(a) Actual base line on the plate.

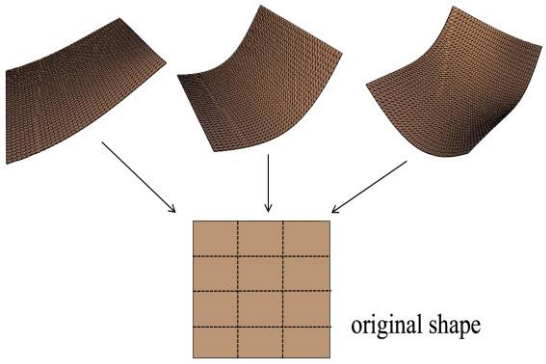

(b) Virtual reference lines

Figure 10. Reference lines on plates

We denote that steel plates are partly stretched or squeezed when they are bended using a press machine. Since the bended plate is not a developable surface, distortion cannot be avoided mathematically. Nevertheless, we can suppose that the sizes of stretch or squeeze are small in our application, because each plate covers only a small part of a large storage tank and the curvature of bended plates is relatively small.

To validate this assumption, we investigated precision by tracking marker positions on a plate. We painted a plate in white, and put nine colored markers on the plate, as shown Figure 11. Then we measured the original shape and bended shapes using a terrestrial laser scanner.

First we manually identified the marker positions on the screen. Each point in a point-cloud has an intensity value, and the colors of points on markers are relatively dark. The marker positions were calculated as the averages of dark points, which were manually selected.

Next we calculated marker positions using automatic mesh flattening methods, which are described later. We mapped points on the curved plate onto the original flat shape, as shown in Figure 10(b), and automatically selected points that were mapped onto markers on the original shape. Each marker position was calculated as the average of selected points.

We compared nine marker positions. In our experiment, the average error of the marker positions was 1.0 mm. This result is practically sufficient for large-scale plates. Our experimental result shows that mesh flattening methods are useful for defining virtual reference lines on steel plates.

4.2 Generation of a mesh model of a plate

In this research, points on a curved plate are mapped onto the original flat shape to determine positions of reference lines. For mapping 3D points on a 2D plane, several mesh flattening methods have been proposed [8-10]. To apply mesh flattening methods, it is necessary to solve linear or non-linear equations with a huge number of variables. When points are densely measured from a steel plate, the necessary memory capacity and calculation time become unacceptably large. Therefore, we generate a simplified mesh for calculating reference lines.

Figure 11. Experiment of virtual makers

In our method, four boundary edges are calculated as B-spline curves using a dense point-cloud. We sampled boundary points on B-spline curves, and then select the adequate number of internal points inside the plate, as shown in Figure 12. Finally, we generate a simplified mesh model using the Delaunay triangulation.

4.3 Mapping points onto a plane

In order to parameterize points on bended plates, points are mapped onto the original flat shape of the plate. We suppose that the original plate is placed on a plane, on which coordinates (u, v) are defined.

Figure 13 shows mapping of boundary points. First, the four corner points are placed at the corner point of the flat plate. Then points on the boundary edge are placed on edges of the original flat plate so that the ratios of distances between points are preserved. These boundary points are fixed and treated as hard constraints for optimization.

Internal points are mapped by optimizing objective functions. Several methods have been proposed for mapping 3D coordinates to a 2D plane. In this research, we apply Harmonic Mapping (HM) [9,11], which is a linear method, and Angle-Based Flattening (ABF) [8], which is a nonlinear method. HM can be applied only to convex shapes, but can be efficiently calculated by solving a linear system. ABF can process any shapes, but is more time-consuming to solve nonlinear equations. In this paper, we implemented these two methods to compare the calculation time and the accuracy.

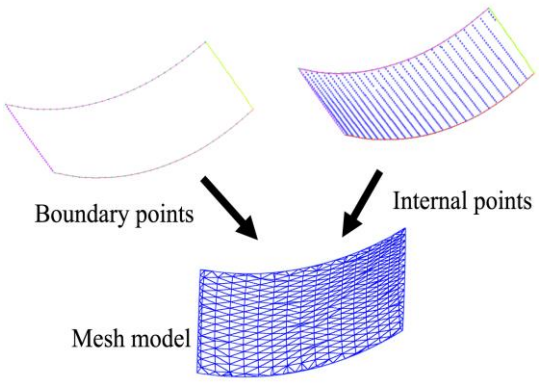

Figure 12. Generation of a simplified mesh model

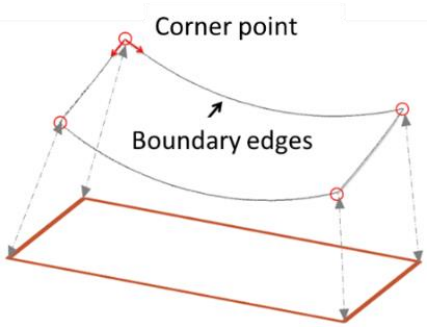

Figure 13. Constraints for flattening

In ABF, as shown in Figure 14(a), flattening is performed so as to approximately preserve the ratios of angles of edges at each vertex. 2D coordinates of vertices in a mesh model can be calculated by solving:

$$\sum_{t\in T}\sum_{i\in V}\frac{1}{\left(\beta_i^t\right)^2}\left(x_i^t-\alpha_i^t\right)^2\rightarrow\min \tag{3}$$

where $\{x_i^t\}$ are angles on the 2D plane, T is a subscript set of triangles, and V is a subscript set of vertices. To solve this optimization, non-linear constraints regarding angles have to be satisfied. ABF calculates this optimization problem using sequential minimal optimization. When angles are calculated, 2D coordinates are calculated using the least squares method.

In HM, an energy term is calculated for each edge connecting two vertices. 2D coordinates $\{\mathbf{p}_i\}$ are calculated by solving the following objective function using parameters in Figure 14(b). This optimization can be efficiently calculated by solving a linear system.

$$\sum_{(i,j)\in E}k_{ij}\left|\mathbf{p}_i-\mathbf{p}_j\right|^2\rightarrow\min$$
$$k_{ij}=\frac{a_{ij}^2+b_{ij}^2-l_{ij}^2}{A_{ij}}+\frac{c_{ij}^2+d_{ij}^2-l_{ij}^2}{B_{ij}} \tag{4}$$

Figure 15 shows examples of flattening using ABF and HM. In either case, almost the same mesh is generated.

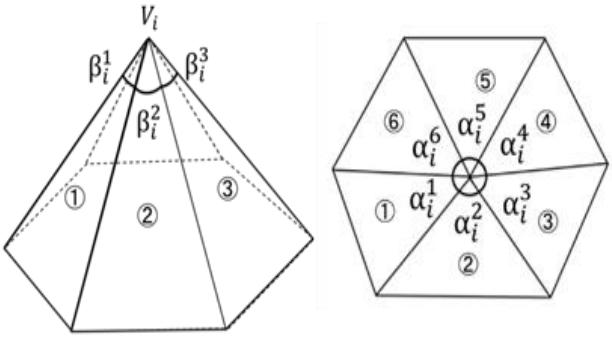

(a) Parameters for ABF

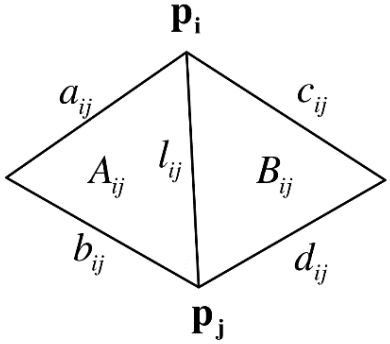

(b) Parameters for HM

Figure 14. Parameters for flattening

4.4 Generation of reference lines

When each point in a mesh model is mapped on the 2D plane, (u,v) parameter is assigned at the point. These parameters are calculated only on the vertices in a simplified mesh. Since each vertex V_i in a mesh model has 3D coordinate (x_i,y_i,z_i) and 2D parameter (u_i,v_i), a B-spline surface can be fit to the mesh model using the least squares method. Figure 16(a) shows a bi-cubic B-spline surface fitted to a mesh model.

Since the rectangle shape in u-v space is the same as the original plate shape, predefined reference lines can be defined in u-v space. Then the reference lines can be mapped onto the bended plate using the equation of the B-spline surface, $(x,y,z)^t=\mathbf{S}(u,v)$. Figure 16(b) shows an example of reference lines generated on a bended plate.

Figure 17 shows reference lines on an actual plate and virtual ones. The both lines are coincident with a sufficient degree of accuracy.

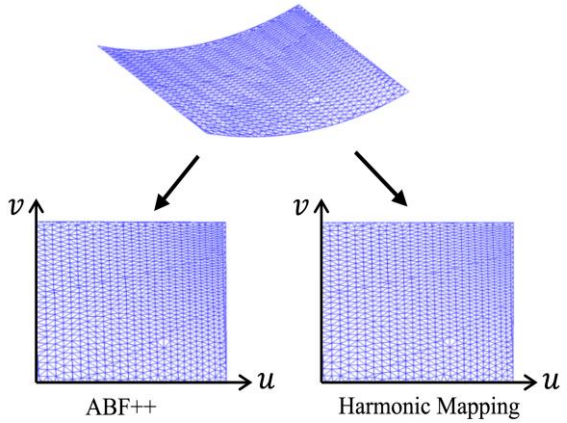

Figure 15. Flattening of a plate mesh

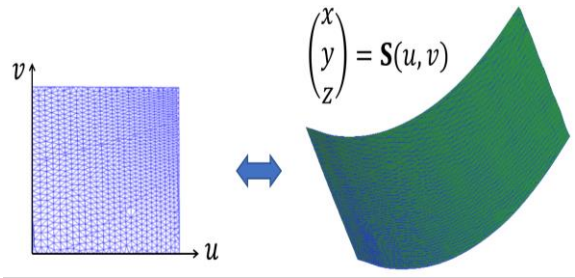

(a) B-spline fitting

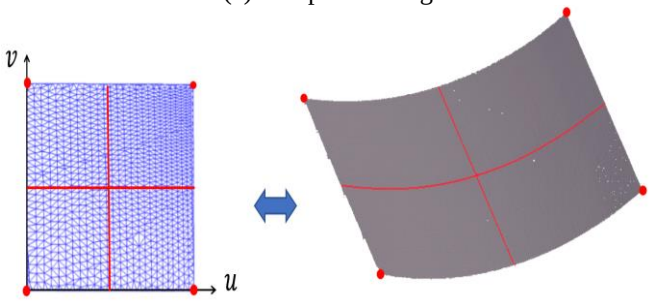

(b) Reference lines on the bended plate

Figure 16. Generation of reference lines

4.5 Visualization of differences in bending process

In our method, arbitrary positions on a plate can be parameterized in u-v space. Therefore, it is possible to compare shapes in every plate-bending phase. We implemented two visualization tools for curvature and displacement.

Figure 18 shows a comparison process. The shapes in different bending steps are mapped in u-v space, and corresponding points are detected. Then a difference map for curvature is generated by calculating curvature values on each shape. In this colored map, unchanged parts are shown in gray. This visualization is helpful for operators to identify what parts are largely bended in the previous operations.

Figure 19 shows displacement maps. In this map, distances between corresponding points are calculated in each bending operation. This visualization is also helpful to understand results of bending operations.

If we maintain point-clouds of plates in all operations, we can analyze tacit knowledge of operators. In constructing large storage tanks, thousands of plates have to be processed by many operators. In our method, we can compare skilled persons to beginners by visualizing sequences of plate bending. The analysis of tacit knowledge is our future work.

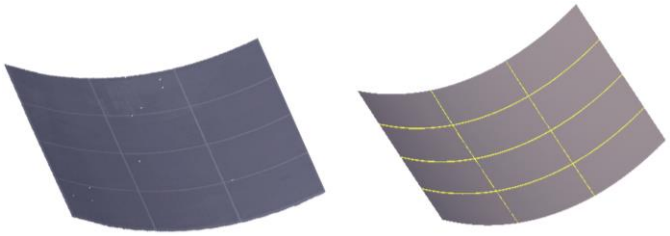

(a) Real reference lines (b) Virtual reference lines

Figure 17. Reference lines on a curved plate

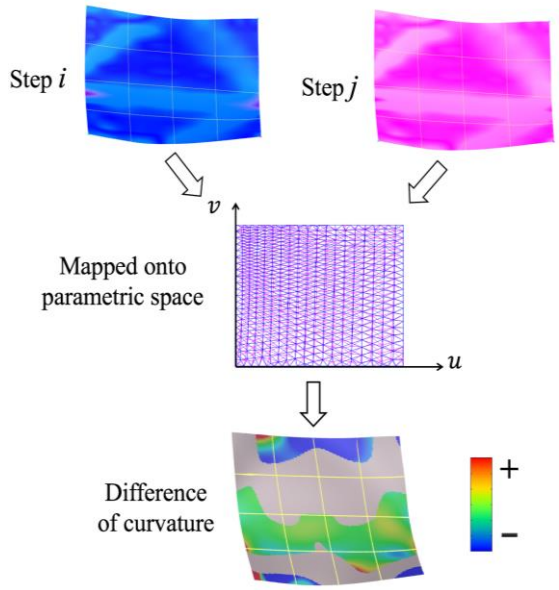

Figure 18. Visualization of curvature differences

5. EXPERIMENTAL RESULTS

We evaluated calculation time of our method. We measured a plate with 4m x 4m using a terrestrial laser scanner, FARO Focus 3D S120. The density of points was 6.3 mm pitch with a distance of 10m. We used a PC with Intel Core i7 3.07 GHz and 12 GB RAM.

Our method consists of the following steps. Table 1 shows calculation time of each step.

(1) Points on a steel plate are extracted from a point-cloud. In this example, the number of extracted points was 277,721.
(2) Four corners and edges of the rectangle plate are calculated.
(3) The mesh model of the plate is generated. In this example, the number of vertices was 10,188.
(4) Points in the mesh model are parameterized using one of ABF and HM methods.
(5) A B-spline surface is fitted to the mesh model for calculating reference lines.

Table 2 shows the total calculation time. Calculation time in both cases is sufficiently short in practical use.

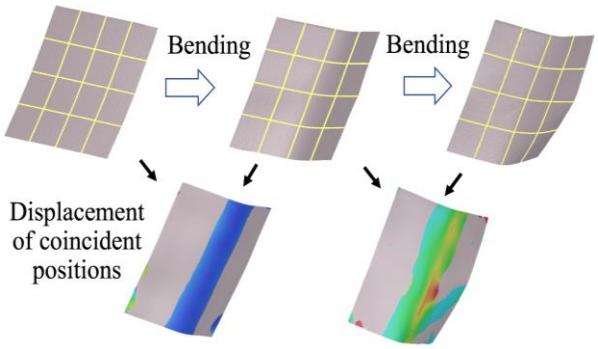

Figure 19. Visualization of displacement

Table 1. Calculation time in each operation

Process	CPU time
(1) Extraction of points on a plate	1.51 sec
(2) Extraction of corners and edges	0.12 sec
(3) Generation of mesh	0.03 sec
(4-1) Parameterization (ABF)	0.71 sec
(4-2) Parameterization (HM)	0.06 sec
(5) B-spline surface fitting	0.05 sec

Table 2. Total calculation time

Case	CPU time
Parameterized by ABF	2.41 sec
Parameterized by HM	1.71 sec

In this example, we reduced the number of vertices to 10,188. We evaluated the scalability by increasing the number of vertices of the simplified mesh. Table 3 shows calculation time of ABF and HM. In HM, the calculation time increases almost in proportion to the number of points, while ABF increases at an accelerated rate. This is because ABF solves the nonlinear optimization problem.

Then we evaluated isometric and equiangular characteristics. We draw a lattice on the original plate as reference lines, and calculated reference lines on the curved plate. Since the original lattice is isometric and equiangular, the reference lines on the curved plate should satisfy these characteristics. We measured d_u, d_v, and θ of all rectangle cells defined on the plate, as shown in Figure 20. Table 4 shows standard deviations of lengths and angles. The errors were sufficiently small. In addition, we evaluated the preciseness of reference lines using the plate in Figure 11. The average errors of each method of ABF and HM were 1.0mm. Since the HM method is more efficient than ABF and the precision is almost same, HM is better than ABF in our applications.

Table 3. Calculation time of parameterization

	Number of points				
	1,000	5,000	10,000	50,000	100,000
ABF	0.04	0.28	0.71	5.89	17.66
HM	0.006	0.02	0.06	0.40	0.84

Table 4. Standard deviation of lengths and angles

	d_u	d_v	Angle θ
ABF	0.8 mm	0.4 mm	0.14 deg
HM	0.8 mm	0.4 mm	0.15 deg

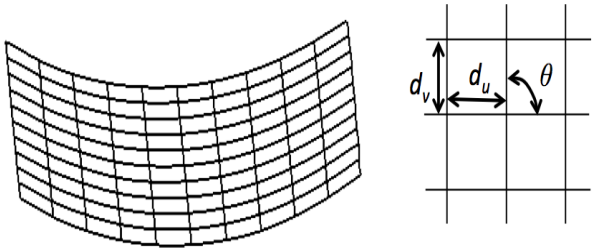

Figure 20. Evaluation of isometric and equiangular characteristics

CONCLUSION

Storage tanks are constructed using many large curved steel plates, which are manufactured from flat plates. In this research, we developed a computer-aided system for supporting plate bending. In our system, 3D shapes are captured using a terrestrial laser scanner, and the amount of modification are sequentially tracked on reference lines defined on the steel plate. In our method, we extracted points on a plate, and identified correspondences between intermediate curved plates and the original flat plate. Then we visualized the differences of shapes and curvatures in each bending step. In our experiments, our method could quickly calculate differences of shapes with practical accuracy.

In future work, we would like to investigate more faithful methods for deciding reference lines. Our method is feasible in practical work, but position errors of reference lines are not small. It may be necessary to correct for the influence of distortion of plates. In addition, measurement with a terrestrial laser scanner is time-consuming compared to point-cloud processing. We would like to investigate more efficient 3D measurement methods.

REFERENCES

1. Lee, J., Kim, C., Son, H, and Kim, C.: Skeleton-Based 3D Reconstruction of As-Built Pipelines from Laser-Scanned Data, ASCE International Conference on Computing in Civil Engineering, 245 (2012)
2. Kawashima, K., Kanai, S., Date, H.: As-Built Modeling of Piping System from Terrestrial Laser Scanned Point Clouds Using Normal-Based Region-Growing, Asian Conference on Design and Digital Engineering, (2013)
3. Masuda, H., Tanaka, I.: Extraction of Surface Primitives from Noisy Large-Scale Point-Clouds, Computer-Aided Design and Applications, 6(3), pp. 387-398 (2009)
4. Masuda, H., Tanaka, I., Matsuoka, R. and Niwa, T.: Reconstruction of Polygonal Faces from Large-Scale Point-Clouds of Engineering Plants, Computer-Aided Design and Applications, 12(5), pp. 555-563 (2015)
5. Sun, J., Hiekata, K., Yamamoto, H., Nakagaki, N., and Sugawara, A.: Efficient Point Cloud Data Processing in Shipbuilding: Reformative Component Extraction Method and Registration Method, IJCC, Journal of Computational Design and Engineering, 1, pp. 202-212 (2014)
6. Joo, H. K., Yazaki, T., Takezawa, M., and Maekawa, T., "Differential geometry properties of lines of curvature of parametric surfaces and their visualization", Graphical Models, 76(4), pp.224-238 (2014)
7. Taubin, G.: A Signal Processing Approach to Fair Surface Design, ACM SIGGRAPH'95 (1995), pp.351-358.
8. Sheffer, A., Lévy, B., Mogilnitsky, M., and Bogomyakov, A.: ABF++: Fast and Robust Angle Based Flattening, ACM Transactions on Graphics, 24(2), 311-330 (2005)
9. Eck, M., DeRose, T., Duchamp, T., Hoppe, H., Lounsbery, M., and Stuetzle, W.: Multiresolution Analysis of Arbitrary Meshes", ACM SIGGRAPH'95, pp.173-182 (1995)
10. Kanai, T., Suzuki, H., and Kimura, F.: Three-Dimensional Geometric Metamorphosis Based on Harmonic Maps, The Visual Computer, 14(4), pp. 166-176 (1998)